AER: Insights 2021, 3(4): 503–522
https://doi.org/10.1257/aeri.20200401

Optimal Lockdown in a Commuting Network[†]

By Pablo D. Fajgelbaum, Amit Khandelwal, Wookun Kim, Cristiano Mantovani, and Edouard Schaal*

We study optimal dynamic lockdowns against COVID-19 within a commuting network. Our framework integrates canonical spatial epidemiology and trade models and is applied to cities with varying initial viral spread: Seoul, Daegu, and the New York City metropolitan area (NYM). Spatial lockdowns achieve substantially smaller income losses than uniform lockdowns. In the NYM and Daegu—with large initial shocks—the optimal lockdown restricts inflows to central districts before gradual relaxation, while in Seoul it imposes low temporal but large spatial variation. Actual commuting reductions were too weak in central locations in Daegu and the NYM and too strong across Seoul. (*JEL* H51, I12, I18, R23, R41)

Commuting networks are the backbone of cities, allowing interactions that are vital for economic growth. On a typical day, Manhattan receives as many commuters as its residents—about 1.6 million people. Two months after the onset of COVID-19, the New York City metropolitan area (NYM) commute flows were 48 percent below pre-pandemic levels. Weighing the economic costs against the benefits of stopping COVID-19, was this reduction too large or not large enough? To fight a highly infectious disease without a vaccine, public authorities must decide if and how to curtail movements across locations connected via commuting and trade.[1] How should lockdown policies be set across locations and time?

In this paper we establish an efficient benchmark against which to measure the losses from uncoordinated or spatially uniform lockdown efforts. We study optimal dynamic lockdowns to fight pandemics in a commuting network using a framework

*Fajgelbaum: Princeton and NBER (email: pfajgelb@princeton.edu); Khandelwal: Columbia GSB and NBER (email: ak2796@columbia.edu); Kim: Southern Methodist University (email: wookunkim@smu.edu); Mantovani: Universitat Pompeau Fabra (email: cristiano.mantovani@upf.edu); Schaal: CREI, ICREA, UPF, BGSE, and CEPR (email: eschaal@crei.cat). Pete Klenow was coeditor for this article. We thank Andy Atkeson for his comments as well as two anonymous referees. Schaal acknowledges financial support from the Spanish Ministry of Economy and Competitiveness, through the Severo Ochoa Programme for Centres of Excellence in R&D (CEX2019-000915-S), the European Research Council under the European Union's Horizon 2020 research and innovation program Starting Grant (804095-OPTNETSPACE), and from the Generalitat de Catalunya, through CERCA and SGR Programme (2017-SGR-1393). We thank SafeGraph for making their data freely available. We thank Hyungmo Choi for providing excellent research assistance.

[†]Go to https://doi.org/10.1257/aeri.20200401 to visit the article page for additional materials and author disclosure statement(s).

[1]Lockdowns were announced fairly uniformly across bordering US states, with a mean difference of four days, although there has been variation in county-level policies. For example, New York, New Jersey, and Connecticut imposed almost simultaneous lockdown in March 2020, while Illinois did so more than two weeks before Missouri (Raifman et al. 2020).

that integrates standard spatial epidemiology and trade models.[2] In the model, a disease spreads through interactions of commuters at the workplace. Lockdown policies directly reduce the real income of workers who stay at home and increase shopping costs and indirectly impact other locations through shifts in expenditures.[3] In reality, policies that close specific businesses preclude commutes along particular routes. Our planning problem determines the fraction of each origin-destination commuting flow allowed to operate at each point in time to minimize the economic costs and the loss of lives. We also implement optimal lockdowns by origin or destination that resemble less flexible closures (e.g., lockdowns by neighborhood).

We apply the model using real-time commuting data across districts in two South Korean cities, Seoul and Daegu, and cell phone mobility data across counties in the NYM. We compare optimal pandemic-fighting strategies across intensities of the initial virus shock and contrast them with the observed commuting responses. We analyze Korean cities because Korea has tested for COVID-19 at greater intensities than most countries, making the timeline of their case data more reliable.[4] Seoul is the largest city in Korea and experienced a relatively small caseload, while Daegu (Korea's fourth-largest city) experienced the country's largest shock. We study the NYM because of its economic importance and rapid spread.

We compute the optimal lockdown given the COVID-19 spread when lockdown policies were announced. The model matches pre-pandemic commuting flows and wages across locations (Korean districts and NYM counties). We estimate the transmission rate using data on the spatial distribution of new cases and commuting flows over time. We use geocoded credit card expenditure data from Seoul to estimate the impact of lockdown on the travel costs of shopping.

Our first results show that in the NYM and Daegu—where the virus initially spread very quickly—locations with high virus-diffusion potential are subject to a strict initial lockdown, eliminating up to 70 percent of pre-pandemic inflows, which is partially relaxed over 3 to 6 months. In the NYM, many locations are locked down early, but only the top three central locations (Manhattan, Brooklyn, and the Bronx) remain closed for a long time in expectation that a vaccine arrives. In contrast, in Seoul—where the initial spread of COVID-19 was much smaller—the planner initially locks down only a few locations of relatively high centrality. As the virus spreads, the lockdown intensifies and retains considerable spatial variation.

Our main result reveals large benefits from spatial targeting. Specifically, we find substantially lower real income losses from spatial targeting compared to an optimal but spatially uniform lockdown. Given the actual case count by April 30, spatial targeting would have led to 20 percent, 32 percent, and 58 percent lower economic costs in Daegu, Seoul, and the NYM, respectively, than the optimal uniform lockdown. We find that optimal lockdowns by destination of commuting flows are

[2] The spatial SIR model we formulate is closely related to the multi-city epidemic model in Arino and van den Driessche (2003), in which the disease is transmitted from infected residents of location i to susceptible residents of location j when they meet in location k. The trade model follows Anderson and van Wincoop (2003).

[3] Caliendo et al. (2018) and Monte, Redding, and Rossi-Hansberg (2018) study diffusion of local shocks across and within cities in related gravity models.

[4] Korea had performed 0.878 tests per one thousand people at the time of its one thousandth patient compared to 0.086 in the United States. Stock (2020), Manski and Molinari (2020), Korolev (2021), and Atkeson (2020a) discuss challenges arising from infrequent testing.

almost as efficient as the fully flexible benchmark, suggesting that spatially targeted business lockdowns may be enough to reap the benefits of spatial targeting.

Finally, we compare the optimal benchmark with the observed commuting reductions resulting from government action and commuters' precautionary behavior. On average across locations, commuting declines reached troughs of 79 percent, 36 percent, and 79 percent below pre-pandemic levels in Daegu, Seoul, and the NYM before modestly reverting upward. In the NYM and Daegu, these city-level declines are not far from the optimal benchmark. However, the most central (peripheral) locations exhibited a weaker (stronger) reduction in commuting than what would have been optimal. Across Seoul, the actual commuting reductions were too strong compared to the optimal. As a result, across all three cities, the real income losses could have been much smaller through optimal spatial targeting.

Studies of optimal epidemic control in economic models include Goldman and Lightwood (2002) and Rowthorn and Toxvaerd (2012) and in the context of COVID-19, Atkeson (2020b); Alvarez, Argente, and Lippi (2020); Jones, Philippon, and Venkateswaran (2020); Piguillem and Shi (2020); Rowthorn (2020); and Rowthorn and Toxvaerd (2020), among others. Acemoglu et al. (2020), Baqaee et al. (2020), and Glover et al. (2020) among others study lockdown with heterogeneous agents.

Adda (2016) demonstrates that diseases spread through transportation networks, exploiting variation from public transport strikes in France, and Viboud et al. (2006) show that work-related flows correlate with influenza's regional spread in the United States. For COVID-19, Tian et al. (2020) argue that the Wuhan lockdown and suspending public transport delayed the spread across China, Fang, Wang, and Yang (2020) show that the lockdown reduced infection rates using real-time movement data, Kissler et al. (2020) show that commuting correlates with cases within New York, and Hsiang et al. (2020) and Flaxman et al. (2020) show that interventions such as lockdown reduced the spread.

Spatial SIR models were first used to study influenza and measles (Rvachev and Longini 1985, Bolker and Grenfell 1995). Germann et al. (2006), Eubank et al. (2004), and Drakopolous and Zheng (2017) study targeted policies in spatial or network models, and Rowthorn, Laxminarayan, and Gilligan (2009) analyze their theoretical properties. For COVID-19, Azzimonti et al. (2020); Birge, Candogan, and Feng (2020); Chang et al. (2020); Chinazzi et al. (2020); and Giannone, Paixão, and Pang (2021) simulate policies in spatial and network SIR models; Argente, Hsieh, and Lee (2020) consider case information disclosure; and Antràs, Redding, and Rossi-Hansberg (2020) study pandemics in a trade model with human interactions.

Our contribution is threefold. First, we implement optimal lockdown over both time and space in a commuting network. Second, to evaluate the diffusion of economic costs through changes in spending, we integrate a general equilibrium trade framework. Third, we use real-time commuting and expenditure data to estimate and compare the actual commuting responses over space with optimal lockdowns.

I. Model

We use a standard spatial epidemiology model similar to Arino and van den Driessche (2003). The general equilibrium corresponds to a standard quantitative

gravity trade model (e.g., Anderson and van Wincoop 2003, and Eaton and Kortum 2002).

A. *Spatial Diffusion*

The economy consists of J locations in continuous time. Before the pandemic, in each location i there are $N_0(i)$ residents, of which a fraction $\lambda(i,j)$ commute to j. We let $\mathbf{\Lambda}$ be the matrix of bilateral commuting flows such that $[\mathbf{\Lambda}]_{ij} = \lambda(i,j)$.[5]

At each time t, the surviving residents of location i are either susceptible, exposed, infected, or recovered in quantities $S(i,t)$, $E(i,t)$, $I(i,t)$, and $R(i,t)$, respectively. Susceptible agents become exposed after interacting with infected agents; exposed agents are latent carriers who do not infect others and become infected at rate γ_I. Infected agents die at rate γ_D or recover (and become immune) at rate γ_R. The spatial distributions are collected in the (column) vectors $\mathbf{S}(t)$, $\mathbf{E}(t)$, $\mathbf{I}(t)$, and $\mathbf{R}(t)$.

The government can control the fraction $\chi(i,j,t)$ of commuting flows from i to j by imposing lockdown measures, providing incentives, or broadcasting information.[6] Every agent is subject to the policy regardless of infection status. Among those not infected and not physically commuting, a fraction δ telecommutes. Among the infected, only the asymptomatic fraction ζ works. The lockdown policies are collected in the J by J matrix $\boldsymbol{\chi}(t)$.

The geographic spread of the disease depends on how much infected and susceptible people interact in space. The infections could happen anywhere at commuting locations, such as in train stations, workplaces, or restaurants. In this benchmark the virus diffuses only through commuting. In alternative specifications we also allow the virus to spread through shopping.

Let $\tilde{S}(j,t) \equiv \sum_{i'} \chi(i',j,t)\lambda(i',j)S(i',t)$ be the number of susceptible agents (from any origin) exposed in j and $\tilde{I}(j,t) \equiv \zeta\sum_{i'} \chi(i',j,t)\lambda(i',j)I(i',t)$ be the number of infected asymptomatic agents (from any origin) spreading the disease in j. In matrix form, $\tilde{\mathbf{S}}(t) \equiv \mathbf{H}_S(t)\mathbf{S}(t)$ and $\tilde{\mathbf{I}}(t) \equiv \mathbf{H}_I(t)\mathbf{I}(t)$, where $\mathbf{H}_S(t)$ and $\mathbf{H}_I(t)$ are spatial incidence matrices that depend on pre-pandemic commuting flows and current lockdown policies:

$$\mathbf{H}_u\big(\chi(t)\big) = \zeta_u\big(\mathbf{\Lambda} \cdot \boldsymbol{\chi}(t)\big)', \tag{1}$$

where $\zeta_I = \zeta$, $\zeta_S = 1$ and $\cdot$ is the element-wise product. The (ji) element of $\mathbf{H}_S(t)$ is the exposure of the $S(i,t)$ susceptible residents of location j to the $\tilde{I}(j,t)$ infected commuters to j. Similarly, the (ji) element of $\mathbf{H}_I(t)$ is the exposure of the $I(i,t)$ infected residents of location j to the $\tilde{S}(j,t)$ susceptible commuters to j.

The flow of new infections in j is

$$M_j\big(\tilde{I}(j,t), \tilde{S}(j,t)\big), \tag{2}$$

[5] These initial distributions could be the equilibrium of a spatial model as in Redding and Rossi-Hansberg (2017). Given our time frame, we assume no job switches other than through lockdown.

[6] An implicit assumption is that policymakers can randomly test to obtain location-specific distributions of each infection status but cannot observe every individual's status. Such random testing would also mitigate potential errors in testing (e.g., Manski and Molinari 2020).

where $M_j(\cdot)$ represents the matching process between infected and susceptible individuals in j. The infections taking place in j are carried back by susceptible and infected agents to their residence. Of these infections, a fraction $H_S(j,i,t)S(i,t)/\tilde{S}(j,t)$ correspond to residents of i. Therefore, the flow of the new infections among location i's residents is

$$\dot{S}(i,t) = -\sum_j \frac{H_S(j,i,t)S(i,t)}{\tilde{S}(j,t)} M_j\big(\tilde{I}(j,t),\tilde{S}(j,t)\big). \tag{3}$$

B. *Real Income*

The economic costs of lockdown enter through the distribution of real income,

$$U(i,t) = \frac{Y(i,t)}{P(i,t)}, \tag{4}$$

where $P(i,t)$ is the cost of living and $Y(i,t)$ is the nominal income of location-i residents:

$$Y(i,t) = \sum_{u=S,E,I,R} \sum_j N_u(i,j,t) w(j,t). \tag{5}$$

Here, $w(j,t)$ is the wage per efficiency unit in j at time t, and $N_u(i,j,t)$ is the flow of efficiency units of type-u commuters from i to j:

$$N_u(i,j,t) = \zeta_u\big[\chi(i,j,t) + \big(1-\chi(i,j,t)\big)\delta\big]\lambda(i,j)u(i,t), \tag{6}$$

for $u = S,E,I,R$, where $\zeta_I = \zeta$ is the fraction of asymptomatic infected and $\zeta_u = 1$ for $u \neq I$. The efficiency units flowing from i to j include those physically commuting, $\chi(i,j,t)$, and those not commuting scaled by the fraction of telecommuters, $\big(1-\chi(i,j,t)\big)\delta$.

The jobs at j produce goods or services with productivity $z(j)$. Consumers have a constant elasticity of substitution σ across goods from different locations. Residents of i face costs $\tau(i,j,t) \equiv \tau\big(i,j,\chi(i,j,t)\big) > 1$ when shopping in j. The lockdown restrictions increase this shopping cost.

At all t, the income of workers employed in j equals the aggregate expenditures in the goods they produce:

$$w(j,t) \sum_{u=S,E,I,R} \sum_i N_u(i,j,t) = \sum_i s(i,j,t) Y(i,t) \quad \text{for all } j, \tag{7}$$

where

$$s(i,j,t) \equiv \left(\frac{p(i,j,t)}{P(i,t)}\right)^{1-\sigma} \tag{8}$$

is the expenditure share of goods from j by residents of location i given the price $p(i,j,t) = \tau(i,j,t)\,w(j,t)/z(j)$, and where

$$P(i,t) = \left(\sum_j p(i,j,t)^{1-\sigma}\right)^{\frac{1}{1-\sigma}} \tag{9}$$

is the price index in i. In equilibrium, $\big\{w(j,t),P(j,t)\big\}$ are such that (7) and (9) hold.

C. *Planning Problem*

A social planner chooses the lockdown matrix to maximize the present discounted value of real income net of loss of lives. The aggregate real income of location j depends on the spatial distributions of lockdown and residents by infection status:

$$U(j,t) \equiv U\big(j;\mathbf{S}(t),\mathbf{E}(t),\mathbf{I}(t),\mathbf{R}(t),\chi(t)\big). \tag{10}$$

A vaccine and a cure become freely available with probability ν in every time period. If the cure occurs at time t, location j generates the real income $\bar{U}(j,t) \equiv U\big(j;0,0,0,\mathbf{S}(t)+\mathbf{E}(t)+\mathbf{I}(t)+\mathbf{R}(t),\mathbf{1}_{J\times J}\big)$ forever. The planning problem is[7]

$$W = \max_{\chi(t)} \int_0^\infty e^{-(r+\nu)t} \sum_j \Big[U(j,t) + \frac{\nu}{r}\bar{U}(j,t) - \omega\gamma_D I(j,t)\Big]\,dt, \tag{11}$$

subject to

$$\dot{\mathbf{S}}(t) = -\mathbf{S}(t)\cdot\Big[\mathbf{H}_S\big(\chi(t)\big)'\Big(\mathbf{M}\big(\tilde{\mathbf{S}}(t),\tilde{\mathbf{I}}(t)\big)\cdot/\tilde{\mathbf{S}}(t)\Big)\Big], \tag{12}$$

$$\dot{\mathbf{E}}(t) = -\dot{\mathbf{S}}(t) - \gamma_I\mathbf{E}(t), \tag{13}$$

$$\dot{\mathbf{I}}(t) = \gamma_I\mathbf{E}(t) - (\gamma_R+\gamma_D)\mathbf{I}(t), \tag{14}$$

$$\dot{\mathbf{R}}(t) = \gamma_R\mathbf{I}(t), \tag{15}$$

where $\mathbf{M}(\cdot)$ is a vector with the new matches, and where $\tilde{\mathbf{S}}(t) = \mathbf{H}_S\big(\chi(t)\big)\mathbf{S}(t)$ and $\tilde{\mathbf{I}}(t) = \mathbf{H}_I\big(\chi(t)\big)\mathbf{I}(t)$ are the susceptible and infected agents.[8] The matrix $\chi(t)$ impacts aggregate real income and the spatial incidence matrix through (1) and (10).

Following standard SEIR models, we impose a multiplicative matching function,

$$M_j\big(\tilde{I},\tilde{S}\big) = \beta_j\tilde{I}\tilde{S}, \tag{16}$$

where β_j is a location-specific diffusion rate. For intuition about the planner's incentives, fix the wage distribution and consider a case where lockdowns do not impact shopping costs. Then the interior solution of the FOC with respect to $\chi(i,j,t)$ is

$$\begin{aligned}(1-\delta)w(j) = {} & \Delta(i,t)\frac{S(i,t)}{N(i,t)}\beta_j\sum_{i'}\zeta I(i',t)\lambda(i',j)\chi(i',j,t) \\ & + \frac{\zeta I(i,t)}{N(i,t)}\beta_j\sum_k \Delta(k,t)S(k,t)\lambda(k,j)\chi(k,j,t),\end{aligned}$$

[7] The flow value for the planner's utility from location j is

$$W_0(j,t) = \big(U(j,t)-\omega\gamma_D I(j,t)\big)dt + \nu dt e^{-rdt}\frac{\bar{U}(j,t)}{r} + e^{-rdt}(1-\nu dt)\,W_0(j,t+dt).$$

This value includes the payoff $U(j,t)-\omega\gamma_D I(j,t)$, the probability νdt of transitioning to a vaccine and its value $\bar{U}(j,t)/r$, and the continuation value. Solving for the present discounted value for location j and adding up across locations yields (11).

[8] The notation $\cdot/$ stands for element-wise ratio.

where $N(i,t)$ is the surviving population of i at time t and $\Delta(i,t) \equiv \mu_S(i,t) - \mu_E(i,t)$, the difference between the co-states of (12) and (13), represents the value of avoiding exposure.

On the left, the economic costs of lockdown equal the wage losses of workers who do not telecommute. On the right, the first line captures the benefits of deterring susceptible agents in i from commuting and therefore being exposed to infected agents at the destination. Similarly, the second line captures that the lockdown deters infected agents from i from transmitting the disease in j. The condition highlights the critical trade-off for the planner: central locations are likely to have higher wages and to be hubs for transmission. So, whether they should endure stricter lockdowns depends on the relative importance of economic and health costs.

II. Data and Parametrization

The parametrization uses case data and real-time commuting flows to estimate the virus transmission rate. The optimization is implemented starting at the lockdown announcement date using pre-pandemic data on commuting flows, wages, population, and spending. Our units of analysis are the 25 districts in Seoul and 8 districts in Daegu. We define the NYM to be 20 counties: 5 NYC boroughs, 5 counties in New York (Putnam, Rockland, Westchester, Nassau, Suffolk), 8 counties in New Jersey (Bergen, Essex, Hudson, Middlesex, Morris, Passaic, Somerset, Union), and 2 counties in Connecticut (Fairfield, New Haven).

A. *Data*

COVID-19 Data.—The Seoul Metropolitan Government released patient-level case data. We filed an Official Information Disclosure Act request to obtain patient-level data from the Daegu Metropolitan Government. We built a daily panel dataset with total confirmed cases in the Seoul and Daegu districts. County-level NYM cases come from Johns Hopkins University and the NY State Department of Health. The Korean data allow us to exclude cases arriving from overseas travels that were stopped at the border.

There are limitations to using data on COVID-19 infections due to bias of the tested population and sensitivity of the tests. These limitations are more severe at the onset of the pandemic when testing intensity was low. Our estimation of the virus transmission rate uses data from the later periods when reporting and testing improved. Additionally, in Korea, testing intensity has been high since the onset.

Daily Commuter Data.—For Seoul, we use district-to-district commute flows on the public transit system (subway and bus) through confidential individual trip-level data (Tmoney 2020). Passengers enter and exit public transit using a card with a unique identifier, from which we obtain the time, origin, and destination of each commute. We retain weekdays from 4:00 AM to 12:00 PM (12:00 PM to 8:00 PM on weekends, since commutes start later) to capture the first commute leg. We aggregate over individual trips to bilateral daily commute flows from January 2018 to April 2020. Pre-pandemic commute flows are the 2018/2019 averages.

For Daegu, we measure daily commuting using subway turnstile data from January 2018 to April 2020, made available by Daegu Metropolitan Transit Corporation. We retain entries and exits using the same commute window as in Seoul. Stations' total entries (exits) plausibly capture the density of residents (jobs) if commuters enter (exit) the subway station closest to their residence (workplace). We aggregate the station-level data to the district level. Pre-pandemic commute flows come from the 2015 Korean Population Census, which records where people live and work (Kim 2020).

For the NYM, we measure county-to-county daily movements using cell phone data from SafeGraph (real-time turnstile data within New York City is not available for suburban commuter rails). The data cover the period from January 1, 2020, to April 30 and are constructed from anonymized smartphone movement data collected daily at the census block group level. We aggregate these data to NYM counties. Pre-pandemic commute flows for the NYM are the averages from January 1 to 20.

Online Appendix Table A.1 summarizes the commuter data and dates of key events described in the next subsection.

Wages and Population.—Population and wage data for the Korean districts come from the 2019 resident registration database and the 2019 Statistical Yearbook of National Tax (Ministry of Interior and Safety of Korea 2019, National Tax Services 2019). NYM county wages are constructed from the 2017 Longitudinal Employer-Household Dynamics Origin-Destination Employment Statistics, which reports the number of workers by wage bin and census block (US Census Bureau 2017).[9] NYM county populations in 2019 are from the US Census Bureau.

Credit Card Spending.—We access data on the universe of transactions at brick-and-mortar shops within Seoul using credit and debit cards from Shinhan Bank, one of Korea's top three banks. We observe the addresses of cardholders and businesses and the purchase values. We construct a daily district-to-district spending matrix from January 2018 to April 2020 among the 25 districts of Seoul, restricting the data to spending by Seoul residents. With this data we estimate elasticities of spending to distance and to post-lockdown commuting flows.

B. *Commuting Responses*

The first three panels in Figure 1 plot time fixed effects for commuting flows relative to pre-pandemic averages since January 2020 in each city. For Seoul and the NYM, where we observe bilateral flows, we estimate $N_{ijt}/\bar{N}_{ij,\tau(t)} = \pi_t + \epsilon_{ijt}$. The dependent variable are flows at t relative to pre-pandemic flows, and $\tau(t)$ is a day-of-week and month dummy. For Daegu the figure reports $E_{it}/\bar{E}_{i,\tau(t)} = \pi_t + \epsilon_{it}$, where the dependent variable is daily turnstile entries. The figure reports π_t for each city.

In each figure the first vertical line denotes the first confirmed case in the country, the middle line denotes the first case in the city, and the last line is the date of

[9] Bins are defined as lower than \$1,250, between \$1,250 and \$3,333, and above \$3,333 per month.

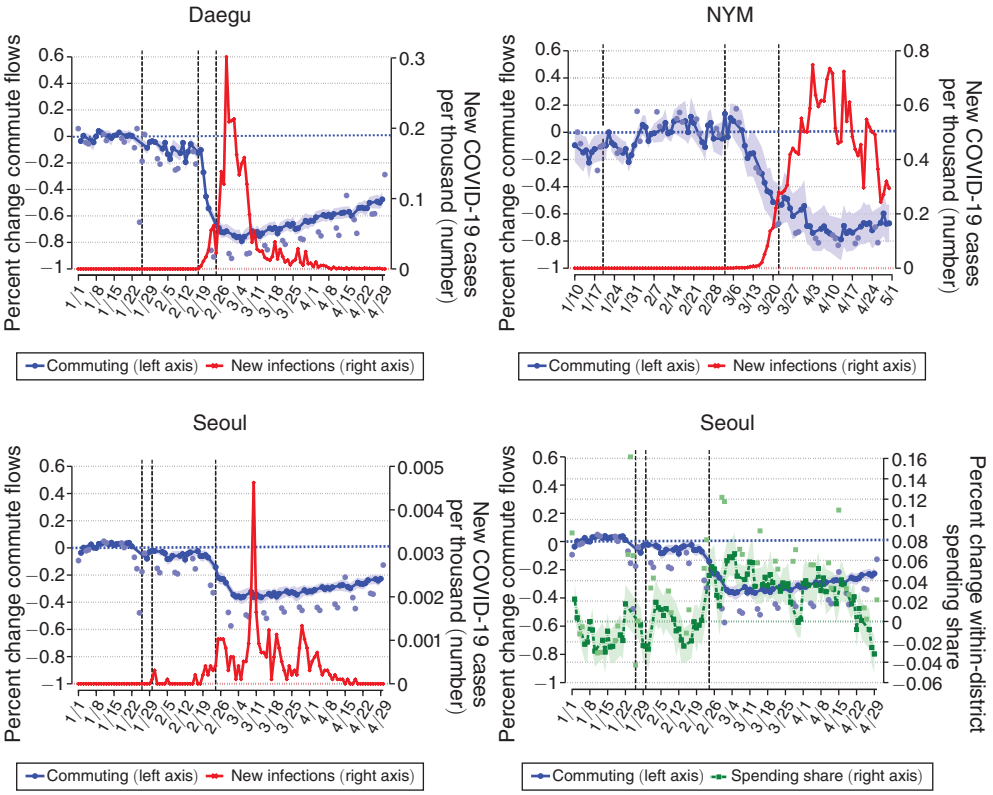

Figure 1. Commute and Spending Responses and Disease Spread

Notes: Figure reports the average daily changes in commute flows relative to the pre-pandemic levels, corresponding to the time fixed effects from the equation in Section IIB (left axis). The time fixed effects are normalized to zero on January 8, 2020, for Daegu and Seoul (January 22, 2020, for the NYM). Weekdays (weekends/holidays) are denoted in darker (lighter) circles. The regression sample size is 968 for Daegu, 75,625 for Seoul, and 48,383 for the NYM. Each observation is a district-by-date pair for Daegu and a district/county-pair-by-date tuple for Seoul and the NYM from January 1, 2020, to April 30. The first vertical line in each graph denotes the date of the first case in the country. The middle and last vertical lines denote the dates of the first case and the lockdown announcement in each city, respectively. Wild bootstrap standard errors are clustered by district for Daegu and two-way clustered by origin and destination for Seoul and the NYM (Cameron, Gelbach, Miller 2008). Error bars show 95 percent confidence intervals. The right axis reports the daily new COVID-19 cases in Daegu (top left), NYM (top right), and Seoul (bottom left). The right axis in the bottom right panel reports the average daily changes in the share of each district's expenditures spent in the same district relative to the pre-pandemic levels, denoted in squares (the commuting response in the bottom right panel is replicated from the bottom left panel).

the lockdown announcement. We overlay the daily counts of new COVID-19 cases scaled by city population.[10]

The first confirmed case within Korea occurred on January 26, and ridership in both cities dropped and remained down roughly 10 percent. After the first confirmed case within Daegu on February 17, the virus spread quickly and commuting declined steeply. Within Seoul, there was no further change after the first confirmed case on

[10] Following Fang, Wang, and Yang (2020), we find a positive correlation between lags of commuting and new daily infections after controlling for location and date fixed effects. See online Appendix B.

January 30. The right axes show that the spread was much larger in Daegu than in Seoul, which may explain the different commuting responses.

After the virus spread throughout Korea during February, a national task force laid out guidelines that included social distancing, working from home, canceling nonessential gatherings, and postponing the start date for schools and universities. Following the announcement on February 24, ridership fell in both cities for roughly two weeks before slowly trending back upward. Overall, ridership fell 60.2 percent and 34.9 percent in Daegu and Seoul, respectively, between the announcement date and April 30. The standard errors suggest similar responses across districts.

In contrast, in the NYM we do not observe declines in commuting before the first confirmed within-city case on March 3. New York State issued a lockdown order on March 22 that closed nonessential businesses.[11] At that time, commuting was already trending downward and continued to fall until mid-April to 67.3 percent below the pre-pandemic flows.

C. *Model Parameters*

We bring the model to the data using daily frequency. Table 1 summarizes the parameters, and Appendix A describes the numerical resolution method.

Disease Dynamics.—Following Ferguson et al. (2020) we set γ_I consistent with an incubation period of 5.1 days and as robustness also consider 4.2 days (Sanche et al. 2020). Following Wang et al. (2020) we set γ_R consistent with a recovery time of 18 days and also show results assuming 10 days. Ferguson et al. (2020) obtain an infection fatality ratio of 0.9 percent, which we use as benchmark, and we also use a lower bound of 0.3 percent across studies (Hall, Jones, and Klenow 2020). Alamian et al. (2019) estimate that 36 percent of infections are asymptomatic. We use this number as benchmark and half that rate as robustness. For δ_u, Dingel and Neiman (2020) report that 46 percent of jobs in the United States could be done from home. A survey by Job Korea says that 60 percent of workers can telecommute.[12] The probability of finding a vaccine corresponds to an expected arrival time of 18 months.

The benchmark value of life ω assumes an expected lifetime of 14.5 years for COVID-19 victims times an annual value of $185,000 calculated by Hall, Jones, and Klenow (2020) minus the discounted value of wages (already accounted for by the planner in the economic costs). To trace a Pareto frontier we also vary ω over a range of values between $1/100$ and 100 times the benchmark. The value of ρ matches an annual interest rate of 4 percent.

[11] New Jersey and Connecticut locked down a few days earlier, but we assign New York's lockdown date.
[12] See http://www.jobkorea.co.kr/GoodJob/Tip/View?News_No=16696, published May 4, 2020.

TABLE 1—SUMMARY OF PARAMETER VALUES

Parameter	Definition	Value	Source
Disease dynamics			
γ_I	Exposed to infected rate	$\{1/5.1, 1/4.2\}$	Ferguson et al. (2020), Sanche et al. (2020)
γ_R	Infected to recovered rate	$\{1/18, 1/10\}$	Wang et al. (2020)
γ_D	Infected to death rate	{0.0005, 0.0002} (see table notes)	Ferguson et al. (2020), Hall, Jones, and Klenow (2020)
ζ	Percent asymptomatic	{0.363, 0.181}	Alamian et al. (2019)
Matching function			
β	Transmission rate (benchmark)	Daegu: 1.58 Seoul: 4.17 NYM: 0.55 Daegu: 0.56	Case data and commuting (see Section IIC)
β (shopping diffusion)	Transmission rate (with shopping)	Seoul: 1.80 NYM: 0.55 Daegu: 0.16	
$\tilde{\beta}$ (shopping diffusion)	Relative transmission via shopping	Seoul: 0.42 NYM: 0.00	
Trade model			
κ_1	Distance-trade cost elast.	0.38	Credit card expenditures (see Section IIC)
κ_0	Scale of trade costs	Daegu: 0.64 Seoul: 1.13 NYM: 0.58	
ε	Lockdown–trade cost elast.	0.11	
σ	Demand elasticity	5	Ramondo, Rodríguez-Clare, and Saborío-Rodríguez (2016)
Other parameters			
δ_I	Telecommuting rate	Korea: 0.62	http://www.jobkorea.co.kr/GoodJob/Tip/View?News_No=16696
		NYM: 0.46	Dingel and Neiman (2020)
ν	Probability of vaccine	$1/(365 \times 1.5)$	Expected time of 1.5 years until vaccine
ω	Value of life	$\{1/100, \ldots, 100\} \times$ (2.6mn − PDV of wages)	Hall, Jones, and Klenow (2020)
ρ	Discount rate	$0.04/365$	

Notes: The table reports the parameters in the benchmark calibration and robustness exercises. The rate γ_D is chosen such that the infection fatality ratio 0.009 equals $\gamma_D/(\gamma_D + \gamma_R)$, and the robustness uses 0.003 instead. See Section IIC for more details.

Matching Function and Transmission Rate.—We assume that, given the number of individuals interacting in a location, contagion is more prevalent in denser districts:[13]

$$\beta_j = \frac{\beta}{area_j}. \tag{17}$$

[13] This adjustment ensures that the aggregate infections are invariant to spatial aggregation. With S susceptible and I infected individuals equally divided among J locations, assuming away spatial interactions, the aggregate number of infections is SI/J, so that slicing a territory reduces infections. Normalizing by area yields instead SI, which is invariant to J.

We set β to match the model-based infection dynamics to COVID-19 case data. Using (3) and (16), the change in the number of susceptible agents is

$$\Delta S(i,t) = -\beta\zeta\left[\sum_j \frac{1}{area_j}\chi(i,j,t)\lambda(i,j)\sum_{i'}\chi(i',j,t)\lambda(i',j)I(i',t)\right]S(i,t) + \varepsilon(i,t), \tag{18}$$

where $\lambda(i,j)$ is the pre-pandemic fraction of residents from i commuting to j at time t, $\chi(i,j,t)$ is the commuting from i to j at time t relative to pre-pandemic flows, and $\varepsilon(i,t)$ accounts for measurement error and other forces driving infections. We observe $\lambda(i,j,t)\chi(i,j,t)$ for Seoul and the NYM, and for Daegu we apply the changes in entries and exits to the pre-pandemic flows to construct its bilateral flows. Note, $S(i,t)$ and $I(i,t)$ are recovered from data on new infections, the calibrated transition rates, and the laws of motion (12) to (14). Given the asymptomatic rate ζ, we set β to minimize the sum of square errors $\sum_i\sum_t \varepsilon(i,t)^2$.

To mitigate concerns that the new-cases data is imprecise and driven by testing, we start the estimation ten days after the peak in new cases in each city. This approach is consistent with the assumptions that the data on new cases became more precise in the latest periods. The results are very similar if we start the estimation at the peak.

Online Appendix Figure A.2 shows that the model replicates well the average number of new cases after the peak in the data and implies a fair amount of dispersion in the dynamics across locations. For the first week after patient zero, the estimation implies a city-level reproduction number (the number of new infections per infected individual) of 1.32 in Seoul, 1.32 in Daegu, and 2.94 in the NYM. These numbers are in line with existing estimates—for example, Shim et al. (2020) estimate 1.5 in Korea, and Fernández-Villaverde and Jones (2020) estimate 2.5 in New York.[14]

Trade Model Parameters.—The bottom right panel of Figure 1 plots $s(i,i,t)$, the share of within-district expenditures, relative to the pre-pandemic levels. Same-district spending shares increase at the time of the lockdown, suggesting that shopping costs increased.

This evidence motivates a specification of trade costs as a function of geographic frictions and lockdown:

$$\tau(i,j,t) \;=\; \kappa_0 distance(i,j)^{\kappa_1}\chi(i,j,t)^{-\varepsilon}. \tag{19}$$

From (8), adding a time subscript and an error term ϵ, we obtain a gravity equation:

$$\begin{aligned}\ln X(i,j,t) \;=\; &\psi(j) + \eta(i) - (\sigma-1)\kappa_1 \ln\big(distance(i,j)\big) \\ &+ (\sigma-1)\varepsilon\ln\big(\chi(i,j,t)\big) + \epsilon(i,j,t),\end{aligned} \tag{20}$$

[14] The reproduction number is the largest eigenvalue of the matrix $\text{diag}\big(\mathbf{S}(t)\big)\mathbf{H}_S'\text{diag}(\beta)\mathbf{H}_I/(\gamma_D+\gamma_R)$ (Diekmann, Heesterbeek, and Metz 1990). Table 1 reports the estimates of β.

where $X(i,j,t)$ are district j's expenditures in goods and services from i at time t, and $\psi(j)$ and $\eta(i)$ are destination and origin fixed effects.[15]

Using the credit card spending data from Seoul, we estimate $(\sigma-1)\kappa_1 = 1.53$ (SE 0.066) and $(\sigma-1)\varepsilon = 0.45$ (SE 0.067).[16] We set $\sigma = 5$ (Ramondo, Rodríguez-Clare, and Saborío-Rodríguez 2016) to recover κ_1 and ε. For each city, we set $z(i)$ and the scale parameter κ_0 to match the pre-pandemic data on wages $w(j)$ and the fraction of same-district expenditures in total expenditures, respectively. The latter is 55 percent in the Seoul credit card data and assumed to be the same across cities.

III. Optimal Spatial Lockdowns

A. *Centrality and Optimal Lockdown*

We implement the model in each city using the case distribution at the lockdown date as the initial condition. The left panel of Figure 2 shows eigenvector centrality by location, which captures the potential by location to diffuse COVID-19 under no lockdown.[17] The right panel shows the fraction of commuting inflows that are optimally shut down.

We find similar qualitative patterns in the NYM and Daegu. The most central locations first experience a strong lockdown, of up to 60 percent in New York and 70 percent in Daegu. In these locations the lockdown is only partially relaxed over three to six months. In the NYM, other locations also exhibit an early lockdown, but only Manhattan remains closed for a long time. In Daegu, all central locations exhibit strict lockdown for a long time.

These patterns contrast with Seoul, where despite the limited spread the planner imposes a long-lasting lockdown to restrain the disease. The planner first locks down a few peripheral locations but maintains economic activity. After the disease has spread, the lockdown intensifies across more central locations.

The results demonstrate that the optimal strategies over time and space depend on the full geography of commute patterns and real income as well as the initial viral spread. When the spread is sufficiently large, the planner first places more weight on shutting down locations that are perceived as transmission hubs, even if they are the main sources of real income. When it is not, those locations are first spared. In either case, the policy maintains a considerable steady-state lockdown to avoid a reemergence of the disease.[18]

[15] Online Appendix Figure A.1 reports positive correlations between commuting and expenditures relative to the pre-pandemic levels, confirming a negative impact of lockdown on shopping.

[16] The results are similar if same-district expenditures are excluded. Monte, Redding, and Rossi-Hansberg (2018) estimate a distance elasticity of 1.29 across Commodity Flow Survey regions.

[17] This is the eigenvector associated with the largest eigenvalue of the matrix $\text{diag}(\mathbf{S}(0))\,\mathbf{H}_S'\mathbf{H}_I$, weighted by the location-specific transmission rate β_j.

[18] The optimal lockdowns are further visualized in online Appendix Figure A.3. The figure shows the lockdown every 30 days. The initial lockdown pattern radiates from geographically central locations and weakens over time.

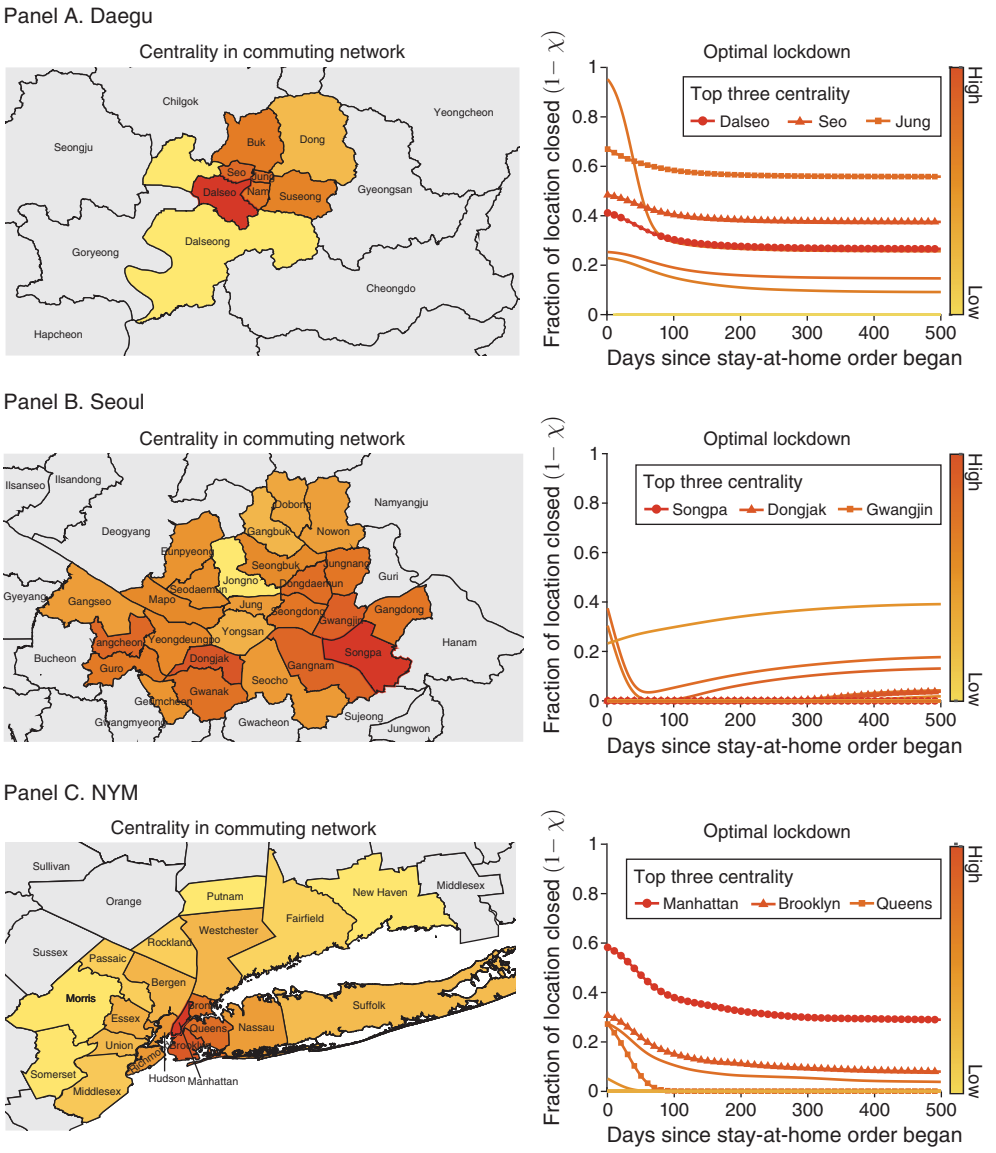

FIGURE 2. CENTRALITY OF COMMUTING LOCATIONS AND OPTIMAL POLICIES

Notes: The left panels denote the (log) centrality of a location (see footnote 17), normalized so that the most central location is one. The right panels plot the optimal policies over time for each location in the network. The color of the line represents the centrality of the location in the network. The three most central locations in the network are indicated in the legend.

B. *Pareto Frontier: Uniform versus Spatially Optimal Lockdown*

We compute a "Pareto" frontier describing the trade-off between cases and economic costs. We solve the optimal lockdown for values of life ω ranging between $1/100$ and 100 times the benchmark. To demonstrate the importance of spatially targeted policies, we also implement optimal uniform lockdown paths, restricted to be constant over space, or optimal lockdowns that vary only by origin

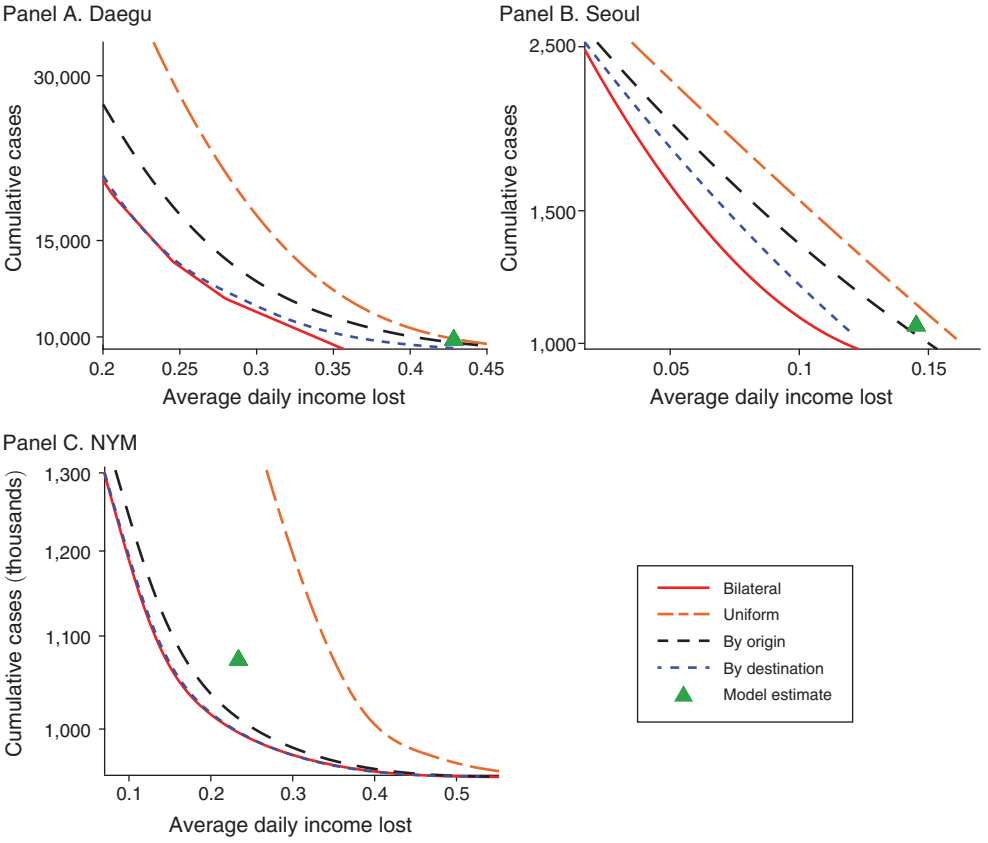

FIGURE 3. PARETO FRONTIERS

Notes: The figures plot the cumulative number of new cases (y-axis, log scale) and the average real income lost per day between the date of the first confirmed case (see online Appendix Table A.1) and April 30, 2020, for parametrizations of the value of life (ω) ranging from $1/100$ to 100 times the benchmark, in the optimal lockdown with space and time variation ("bilateral"), in the spatially uniform optimal solution with time variation only ("uniform," the same lockdown across all locations), and in the optimal solution where only origin or destination can be closed ("by origin" and "by destination," respectively). The green triangle shows the case count and real income lost implied by the estimated model on April 30, 2020.

and destination. Figure 3 plots cumulative COVID-19 cases against the economic loss since the pre-pandemic period at the last period of our data (April 30) across these values of ω, along with the actual economic costs and cases in the estimated model.

We find large gains from implementing optimal spatial lockdown. Compared to uniform optimization, given the actual number of cases, spatially targeted lockdown leads to 20 percent, 32 percent, and 58 percent lower economic costs in Daegu, Seoul, and the NYM, respectively. In the NYM and Daegu, the gap in economic cost between uniform and optimal policies grows for higher values of life.

The actual economic costs and cumulative cases were far from the optimal but close to the space-blind optimal policy. Under spatial targeting, the same number of cumulative cases could have been reached at 19 percent, 27 percent, and 37 percent

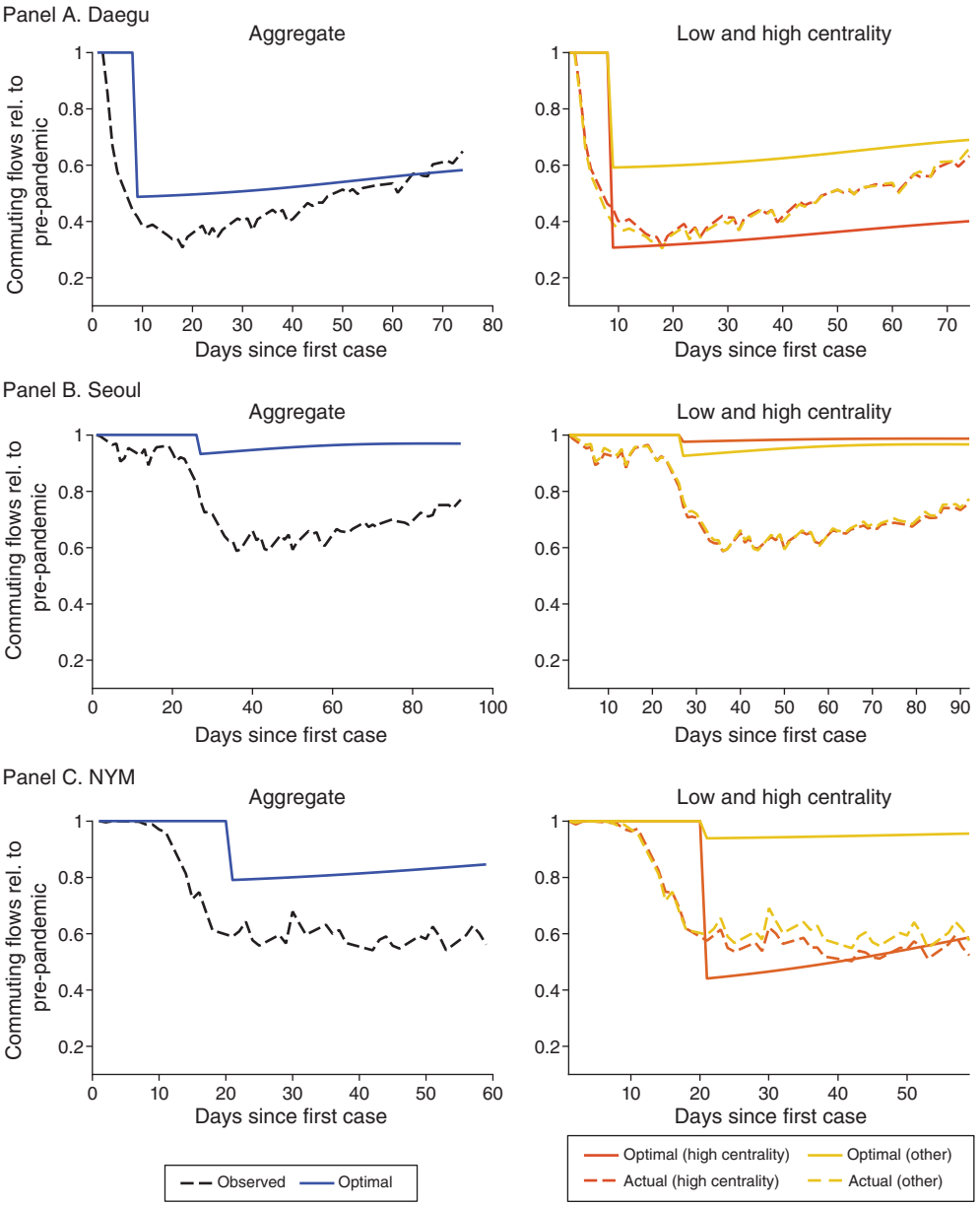

FIGURE 4. CHANGES IN COMMUTING FLOWS: OPTIMAL AND OBSERVED

Notes: In the left panels, the dashed black line shows the aggregate commuting flows in each city starting from the date of the first confirmed case in each city. The solid and circled blue lines show the aggregate commuting flows implied by the optimal spatial policy. In the right panels, optimal and observed commuting responses are divided by the top three central locations (darker shade) and the other locations.

lower economic costs in Daegu, Seoul, and the NYM, respectively. The gains from optimal lockdowns by destination are larger than by origin and very close to the benchmark, suggesting that business lockdowns may be enough to reap the benefits of spatial targeting.

C. *Optimal and Observed Commuting Reductions*

We now compare observed reductions in commuting with the model's optimal flows. The left panel of Figure 4 shows aggregate commuting relative to pre-pandemic values in the data and under optimal lockdown. Since the optimal policies are implemented at the time of lockdown, they are shown as a flat line until that time. The right panel shows inflows for high- and low-centrality locations. In Daegu and the NYM, the actual city-level reductions in commuting were not very far from the optimal benchmark. In New York, a 40 percent drop took place during the time leading up to the lockdown. In the model, the optimal lockdown in that period is about 20 percent. We find an even closer pattern in Daegu, where the optimal lockdown is weakly relaxed over time, as in the data. However, the most central (peripheral) locations of both the NYM and Daegu exhibited a weaker (stronger) reduction in commuting than the optimal. In Seoul, the actual reductions were much stronger than at the optimal in all locations. These differences explain why the estimated economic costs from actual commuting responses were larger than the spatially optimal ones, as in Figure 3.

D. *Alternative Specifications*

Online Appendix Figure A.5 shows that spatial lockdown patterns are robust to the alternative parametrizations described in the previous section. Figure A.6 shows that for a large shock affecting 1 percent of the population, or for a value of life equal to 100 times the benchmark, the qualitative patterns in Seoul resemble those in Daegu and the NYM.

We also implement a case where the virus diffuses through shopping. Agents from i now interact with other agents in location j at rate $\chi(i,j,t)\lambda(i,j) + \tilde{\beta}q\big(i,j,t,\chi(t)\big)$, where $q(i,j,\cdot,\cdot)$ is their per capita consumption of goods from j and $\tilde{\beta}$ is the intensity of diffusion through shopping relative to commuting. Table 1 shows the parameter estimates, and online Appendix Figures A.7 to A.9 replicate the lockdown policies and Pareto frontier in this case. Compared to the benchmark, the lockdown is weaker in Daegu and Seoul due to the smaller estimate of β. However, the qualitative spatial patterns of lockdown and the magnitude of the gains from targeted spatial lockdown implied by the Pareto frontier are similar.

IV. Conclusion

Our framework could be applied to other spatial scales such as across cities, states, or countries and to study the optimal spatial deployment of a vaccine in limited supply. Future work could also relax the assumption that worker-job matches are kept constant by allowing for potentially sluggish job reallocations as lockdowns unwind.

REFERENCES

Acemoglu, Daron, Victor Chernozhukov, Iván Werning, and Michael D. Whinston. 2020. "A Multi-Risk SIR Model with Optimally Targeted Lockdown." NBER Working Paper 27102.

Adda, Jérôme. 2016. "Economic Activity and the Spread of Viral Diseases: Evidence from High-Frequency Data." *The Quarterly Journal of Economics* 131 (2): 891–941.

Alamian, A., S. Pourbakhsh, A. Shoushtari, and H. Keivanfar. 2019. "Seroprevalence Investigation of Newcastle Disease in Rural Poultries of the Northern Provinces (Golestan, Gilan, and Mazandaran) of Iran." *Archives of Razi Institute* 74 (4): 365–73.

Alvarez, Fernando E., David Argente, and Francesco Lippi. 2020. "A Simple Planning Problem for COVID-19 Lockdown." NBER Working Paper 26981.

Anderson, James E., and Eric van Wincoop. 2003. "Gravity with Gravitas: A Solution to the Border Puzzle." *American Economic Review* 93 (1): 170–92.

Antràs, Pol, Stephen J. Redding, and Esteban Rossi-Hansberg. 2020. "Globalization and Pandemics." NBER Working Paper 27840.

Argente, David O., Chang-Tai Hsieh, and Munseob Lee. 2020. "The Cost of Privacy: Welfare Effect of the Disclosure of COVID-19 Cases." NBER Working Paper 27220.

Arino, Julien, and P. van den Driessche. 2003. "A Multi-City Epidemic Model." *Mathematical Population Studies* 10 (3): 175–93.

Atkeson, Andrew. 2020a. "How Deadly is COVID-19? Understanding the Difficulties with Estimation of its Fatality Rate." NBER Working Paper 26965.

Atkeson, Andrew. 2020b. "What Will be the Economic Impact of COVID-19 in the US? Rough Estimates of Disease Scenarios." NBER Working Paper 26867.

Azzimonti, Marina, Alessandra Fogli, Fabrizio Perri, and Mark Ponder. 2020. "Pandemic Control in Econ-Epi Networks." NBER Working Paper 27741.

Baqaee, David, Emmanuel Fahri, Michael J. Mina, and James H. Stock. 2020. "Reopening Scenarios." NBER Working Paper 27244.

Birge, John R., Ozan Candogan, and Yiding Feng. 2020. "Controlling Epidemic Spread: Reducing Economic Losses with Targeted Closure." Becker Friedman Institute Working Paper 2020-57.

Bolker, Benjamin, and Bryan Thomas Grenfell. 1995. "Space, Persistence and Dynamics of Measles Epidemics." *Philosophical Transactions of the Royal Society of London. Series B: Biological Sciences* 348 (1325): 309–20.

Caliendo, Lorenzo, Fernando Parro, Esteban Rossi-Hansberg, and Pierre-Daniel Sarte. 2018. "The Impact of Regional and Sectoral Productivity Changes on the US Economy." *The Review of Economic Studies* 85 (4): 2042–2096.

Cameron, A., Jonah Gelbach, and Douglas Miller. 2008. "Bootstrap-Based Improvements for Inference with Clustered Errors." *Review of Economics and Statistics* 90 (3): 414–27.

Chang, Serina, Emma Pierson, Pang Wei Koh, Jaline Gerardin, Beth Redbird, David Grusky, and Jure Leskovec. 2020. "Mobility Network Models of COVID-19 Explain Inequities and Inform Reopening." *Nature* 589 (7840) 82–87.

Chinazzi, Matteo, Jessica T. Davis, Marco Ajelli, Corrado Gioannini, Maria Litvinova, Stefano Merler, Ana Pastor y Piontti, et al. 2020. "The Effect of Travel Restrictions on the Spread of the 2019 Novel Coronavirus (COVID-19) Outbreak." *Science* 368 (6489): 395–400.

Daegu Metropolitan Transit Corporation. 2020. "Hourly Number of Entries and Exits by Stations (2018–2020)." https://www.data.go.kr/dataset/15002503/fileData.do (accessed May 11, 2020).

Diekmann, O., J. A. P. Heesterbeek, and J. A. Metz. 1990. "On the Definition and the Computation of the Basic Reproduction Ratio R0 in Models for Infectious Diseases in Heterogeneous Populations." *Journal of Mathematical Biology* 28 (4): 365–82.

Dingel, Jonathan I., and Brent Neiman. 2020. "How Many Jobs Can Be Done at Home?" NBER Working Paper 26948.

Drakopolous, Kimon, and Fanyin Zheng. 2017. "Network Effects in Contagion Processes: Identification and Control." Columbia Business School Research Paper 18-8.

Eaton, Jonathan, and Samuel Kortum. 2002. "Technology, Geography, and Trade." *Econometrica* 70 (5): 1741–779.

Eubank, Stephen, Hasan Guclu, V. S. Anil Kumar, Madhav V. Marathe, Aravind Srinivasan, Zoltán Toroczkai, and Nan Wang. 2004. "Modelling Disease Outbreaks in Realistic Urban Social Networks." *Nature* 429 (6988): 180–84.

Fajgelbaum, Pablo D., Amit Khandelwal, Wookun Kim, Cristiano Mantovani, and Edouard Schaal. 2021. "Replication Data for: Optimal Lockdown in a Commuting Network." American Economic Association [publisher], Inter-university Consortium for Political and Social Research [distributor]. https://doi.org/10.3886/E127341V1.

Fang, Hanming, Long Wang, and Yang Yang. 2020. "Human Mobility Restrictions and the Spread of the Novel Coronavirus (2019-nCoV) in China." NBER Working Paper 26906.

Ferguson, N., D. Laydon, G. Nedjati Gilani, N. Imai, K. Ainslie, M. Baguelin, S. Bhatia, et al. 2020. *Report 9: Impact of Non-Pharmaceutical Interventions (NPIs) to Reduce COVID-19 Mortality and Healthcare Demand*. Technical report, Imperial College London. https://doi.org/10.25561/77482.

Fernández-Villaverde, Jesús, and Charles I. Jones. 2020. "Estimating and Simulating a SIRD Model of COVID-19 for Many Countries, States, and Cities." NBER Working Paper 27128.

Flaxman, S., S. Mishra, A. Gandy, H. J. T. Unwin, T. A. Mellan, H. Coupland, C. Whittaker, et al. 2020. "Estimating the Effects of Non-Pharmaceutical Interventions on COVID-19 in Europe." *Nature* 584: 257–61.

Germann, Timothy C., Kai Kadau, Ira M. Longini Jr., and Catherine A. Macken. 2006. "Mitigation Strategies for Pandemic Influenza in the United States." *Proceedings of the National Academy of Sciences* 103 (15): 5935–940.

Giannone, Elisa, Nuno Paixão, and Xinle Pang. 2021. "JUE Insight: The Geography of Pandemic Containment." *Journal of Urban Economics*. https://doi.org/10.1016/j.jue.2021.103373.

Glover, Andy, Jonathan Heathcote, Dirk Krueger, and José-Víctor Ríos-Rull. 2020. "Health versus Wealth: On the Distributional Effects of Controlling a Pandemic." Human Capital and Economic Opportunity Working Group Working Paper 2020-038.

Goldman, Steven Marc, and James Lightwood. 2002. "Cost Optimization in the SIS Model of Infectious Disease with Treatment." *Topics in Economic Analysis & Policy* 2 (1): 1007.

Hall, Robert E., Charles I. Jones, and Peter J. Klenow. 2020. "Trading Off Consumption and COVID-19 Deaths." *Federal Reserve Bank of Minneapolis Quarterly Review* 42 (1): 2–13.

Hsiang, Solomon, Daniel Allen, Sébastien Annan-Phan, Kendon Bell, Ian Bolliger, Trinetta Chong, Hannah Druckenmiller, et al. 2020. "The Effect of Large-Scale Anti-Contagion Policies on the COVID-19 Pandemic." *Nature* 585 (7824): E7.

Johns Hopkins University. 2020. "COVID-19 Data Repository by the Center for Systems Science and Engineering (CSSE) at Johns Hopkins University." https://coronavirus.jhu.edu/map.html (accessed May 2020).

Jones, Callum J., Thomas Philippon, and Venky Venkateswaran. 2020. "Optimal Mitigation Policies in a Pandemic: Social Distancing and Working from Home." NBER Working Paper 26984.

Kim, Wookun. 2020. "The Valuation of Local Government Spending: Gravity Approach and Aggregate Implications." UCLA Ziman Center Working Paper 2020-001.

Kissler, Stephen M., Nishant Kishore, Malavika Prabhu, Dena Goffman, Yaakov Beilin, Ruth Landau, Cynthia Gyamfi-Bannerman, et al. 2020. "Reductions in Commuting Mobility Correlate with Geographic Differences in SARS- CoV-2 Prevalence in New York City." *Nature Communications* 11 (1): 4674.

Korolev, Ivan. 2021. "Identification and Estimation of the SEIRD Epidemic Model for COVID-19." *Journal of Econometrics* 220 (1): 63–85.

Manski, Charles F., and Francesca Molinari. 2020. "Estimating the COVID-19 Infection Rate: Anatomy of an Inference Problem." *Journal of Econometrics* 220 (1): 181–92.

Ministry of Interior and Safety of Korea. 2019. "Resident Registration Population Statistics." https://27.101.213.4/# (accessed May 11, 2020).

Monte, Ferdinando, Stephen J. Redding, and Esteban Rossi-Hansberg. 2018. "Commuting, Migration, and Local Employment Elasticities." *American Economic Review* 108 (12): 3855–90.

National Tax Services. 2019. *2019 Statistical Yearbook of National Tax.* Ministry of Economy and Finance of Korea.

NY State Department of Health. 2020. "New York State Statewide COVID-19 Testing." https://health.data.ny.gov/Health/New-York-State-Statewide-COVID-19-Testing/xdss-u53e (accessed May 2020).

Piguillem, Facundo, and Liyan Shi. 2020. "The Optimal COVID-19 Quarantine and Testing Policies." CEPR Discussion Paper 14613.

Raifman, J., K. Nocka, D. Jones, J. Bor, S. Lipson, J. Jay, and P. Chan. 2020. "COVID-19 US State Policy Database." Ann Arbor, MI: Inter-university Consortium for Political and Social Research.

Ramondo, Natalia, Andrés Rodríguez-Clare, and Milagro Saborío-Rodríguez. 2016. "Trade, Domestic Frictions, and Scale Effects." *American Economic Review* 106 (10): 3159–84.

Redding, Stephen J. and Esteban Rossi-Hansberg. 2017. "Quantitative Spatial Economics." *Annual Review of Economics* 9: 21–58.

Rowthorn, Robert 2020. "A Cost-Benefit Analysis of the COVID-19 Disease." *Oxford Review of Economic Policy.* doi:10.1093/oxrep/graa030.

Rowthorn, Robert, Ramanan Laxminarayan, and Christopher A. Gilligan. 2009. "Optimal Control of Epidemics in Metapopu lations." *Journal of the Royal Society Interface* 6 (41): 1135–144.

Rowthorn, Robert, and Flavio Toxvaerd. 2012. "The Optimal Control of Infectious Diseases via Prevention and Treatment." CEPR Discussion Paper 8925.

Rowthorn, Robert, and Flavio Toxvaerd. 2020. "The Optimal Control of Infectious Diseases via Prevention and Treatment." Cambridge Working Papers in Economics 2027.

Rvachev, Leonid A., and Ira M. Longini Jr. 1985. "A Mathematical Model for the Global Spread of Influenza." *Mathematical Biosciences* 75 (1): 3–22.

SafeGraph. 2020. "Social Distancing Metrics Dataset." https://docs.safegraph.com/docs/social-distancing-metrics (accessed May 2020).

Sanche, Steven, Yen Ting Lin, Chonggang Xu, Ethan Romero-Severson, Nick Hengartner, and Ruian Ke. 2020. "High Contagiousness and Rapid Spread of Severe Acute Respiratory Syndrome Coronavirus 2." *Emerging Infectious Diseases* 26 (7): 1470–477.

Seoul Metropolitan Government. 2020. "COVID-19 Dashboard." https://www.seoul.go.kr/coronaV/coronaStatus.do (accessed May 11, 2020).

Shim, Eunha, Amna Tariq, Wongyeong Choi, Yiseul Lee, and Gerardo Chowell. 2020. "Transmission Potential and Severity of COVID- 19 in South Korea." *International Journal of Infectious Diseases* 93: 339–44.

Shinhan Bank. 2020. "District-to-District Credit Card Spending in Seoul (2018–2020)."

Stock, James H. 2020. "Data Gaps and the Policy Response to the Novel Coronavirus." NBER Working Paper 26902.

Tian, Huaiyu, Yonghong Liu, Yidan Li, Chieh-Hsi Wu, Bin Chen, Moritz U. G. Kraemer, Bingying Li, et al. 2020. "An Investigation of Transmission Control Measures during the First 50 Days of the COVID-19 Epidemic in China." *Science* 368 (6491): 638–42.

Tmoney. 2020. "Seoul Public Transportation and Subway Data (2018–2020)." Seoul Big Data Campus, Seoul, South Korea.

US Census Bureau. 2010–2019. "County Population Totals 2010–2019." https://www.census.gov/data/datasets/time-series/demo/popest/2010s-counties-total.html (accessed March 2020).

US Census Bureau. 2017. "LEHD Origin-Destination Employment Statistics–LODES7." https://lehd.ces.census.gov/data/ (accessed March 2020).

Viboud, Cécile, Ottar N. Bjørnstad, David L. Smith, Lone Simonsen, Mark A. Miller, and Bryan T. Grenfell. 2006. "Synchrony, Waves, and Spatial Hierarchies in the Spread of Influenza." *Science* 312 (5772): 447–51.

Wang, Huwen, Zezhou Wang, Yinqiao Dong, Ruijie Chang, Chen Xu, Xiaoyue Yu, Shuxian Zhang, et al. 2020. "Phase-Adjusted Estimation of the Number of Coronavirus Disease 2019 Cases in Wuhan, China." *Cell Discovery* 6 (10).